International Journal of Engineering & Technology, 7 (4.30) (2018) 527-532

International Journal of Engineering & Technology

Website: www.sciencepubco.com/index.php/IJET

Research paper

Application of Caputo-Fabrizio Fractional Order Derivative (NFD_t) in Simulating the MHD Flow of the Third Grade non-Newtonian Fluid in the Porous Artery

Salah Uddin1*, M. Mohamad[1], Suliadi Sufahani[1], MGhazali Kamardan[1], Obaid Ullah Mehmood[2], Fazli Wahid[3] and R. Roslan[1]

[1]*Department of Mathematics and Statistics, Faculty of Applied Sciences and Technology, Universiti Tun Hussein Onn Malaysia, Pagoh Educational Hub,84600 Pagoh, Johor, Malaysia*

[2]*Faculty of Science, Deprartment of Mathematics, Comsats Institute of Information Technology, Wah Cantt, 47040, Pakistan*

[3]*Faculty of computer science and Information Technology, Universiti Tun Hussein Onn Malaysia, , 86400 Batu Pahat, Johor, Malaysia*

**Corresponding author E-mail: salahuddinjalil@gmail.com*

Abstract

In this paper, the third grade non-Newtonian MHD blood flow in the porous arteries subjected to the periodic pressure gradient was studied using the Caputo-Fabrizio (NFDt) time fractional order derivative. The time fractional model was solved by taking the Laplace and the finite Hankel transforms. Results were compared with those reported in the previous studies and good agreement was found. The Mathematica software was used to simulate the velocity profile and the Bessel functions with zero order and first order of first kind. The correlations between the flow velocity and the third grade non-Newtonian fluid parameter, the magnetic field and the porosity were negative. Nevertheless, the flow velocity increased with respect to the Womersely number.

Keywords: *Caputo-Fabrizio fractional derivative, Incompressible fluid, Unsteady pulsatile.*

1. Introduction

Blood flows inside human arteries consist of red blood cells (RBCs), white blood cells (WBCs), platelets and other nutrients. Blood serves as a carrier in transporting water, glucose, minerals and other necessary materials, etc. to organs. Several artery properties such as wall porosity, wall elasticity and phase angle could affect the blood flow behavior. RBC is rich in iron; therefore, its behavior is sensitive to the magnetic field. The MHD blood flow simulation using the local and time fractional models has been extensively reported. According to Abdullah et al [1], the velocities of blood and magnetic particles were low in the presence of external magnetic field. However, both velocities increased when the Reynolds number decreased. According to Akbar [2], for symmetric stenosis, the resistance caused by impedance reaches to its maximum value, and due to high flow rate in the diverging tapered artery it was smaller than as compared to the converging tapered artery case and size of the trapping bolus was increased by increasing the height of the stenosis δ and n, while the number and size of the trapped bolus was decreased in the non-tapered artery $\phi = 0$ and converging tapered artery $\phi < 0$ than as compared to the diverging tapered artery $\phi > 0$. Akbar and Nadeem [3] found that by simply increasing the Weissenberg number, the fluid velocity increased and the impedance resistance decreased. The flow velocity in the converging tapered artery was higher than those in the non-tapered and diverging tapered arteries. Also, by increasing m, n and L, the resistence to impedance increased for all arteries. In Akbarzadeh [4] reported that, the effect of viscous forces on blood flow was more evident at low Womersley number; all velocity plots were parabolic in shape and oscillation of flow velocity was found due to the pressure gradient. Furthermore, in the presence of high pressure gradient, the velocity remained constant at the extreme positions and it was higher in the core region. Akinshilo and Sobamowo [5] have established various MHD fluid flow models, by taking into account the thermophoresis parameters and viscosity. Their results were useful for the treatment of blood-related diseases by improving the drug delivery mechanism and the blood transportation in the porous medium via nano particles. According to Bao et al [6], their non-contact technique (in which the free surface flow of liquid oxygen was controlled by employing the non-uniform magnetic field) could develop the interface renewal and, minimize the resistance of flow inside the cryogenic distillation column by refining the flow uniformity, (more effective than air separation of cryogenic). According to Das [7] highlighted that increased viscoelastic parameter would decrease the flow velocity. However, by increasing the porosity and the mass Garashof number, the flow velocities of both Newtonian and non-Newtonian fluids increased significantly. The effect of viscoelastic parameter on wall shear stress was more evident than those on temperature and concentration profiles. Eldesoky [8] reported that both channel temperature and axial blood flow velocity increased with respect to the Prandtl number and the heating source parameter. However, these parameters decreased as, the decay's parameter increased. The normal blood flow velocity decayed as the Prandtl number and the heating source parameter increased. The results were useful for physiological fluid dynamists and medical practitioners. The temperature variation in the radial direction was marginal as reported by Fardad et al [9], however, it had a pseudo parabolic propensity upon normalization. Gupta et al [10], highlighted that the wall shear stress in the irreg-

ular stenotic region for *Re* = 130 – 540 was unstable. Krasnov et al [11] reported that the flow model transformations were significantly affected by the magnetic field. They have adopted the finite difference approximation and the conservative scheme approach to simulate the turbulent flow subjected to moderate magnetic field. According to them, this scheme was more stable and accurate than the upwind discretization approach. The method presented by Mekheimer and Kot [12] was not applicable for vessel constriction $\delta/R_0 << 1$ as the fully developed flow equations were used (which was suitable for Poiseuillle-like flow). As reported by them, the flow velocity predicted by using the Newtonian fluid model was higher than that of the particle fluid suspension model. Furthermore, the axial velocity curve for the non-curvature artery had higher transmission than that of the curvature one. Okuyade [13] reported that velocity, pressure and temperature distributions were diminished by the blood viscosity. Parmar and Jain [14] claimed that the heat transfer rate increased with respect to the radiation and Eckert numbers. As compared to the Newtonian, Casson and Williamson fluid models, the Maxwell fluid model exhibited a more effective and satisfactory thermal heat transfer capacity. Furthermore, in the presence of strong external magnetic field, the momentum of the boundary layer diminished and the thermal boundary layer thickened. Factors such as Schmidt, Hartmann, Grashof, Eckert numbers and the chemical reaction parameters had no significant effects on the temperature profiles as reported by Ram et al [15]. However, the fluid velocity was strongly affected by all factors, except the Hartmann number. Both permeability and frequency parameters affect the temperature and the velocity profiles. There was a remarkable decrease in the velocity by increasing S_c and E_c, whereas the temperature and velocity decreased as the rising the radiation parameter increased. The increase of transmural pressure by increasing the radial velocity could cause the overthrow of LDL at the maximum height of the stenosis. This condition would lead to the intimal stiffening of the artery in the particular region as reported by Singh and Rathee [16]. By increasing the pressure gradient, there was a rise/drop in the systolic/diastolic pressures, which was undesirable for patients suffering from heart diseases. The blood flow near the maximum height of the stenosis was disturbed due to the increasing wall shear stress. The intensity of magnetic field should be carefully adjusted. Venkateswarlu and Rao [17] increased the hematocrit values increasing the pressure gradient. They highlighted that both systolic and diastolic pressures should be bounded.

In the present research, the MHD blood flow through a porous artery of pulastile nature was simulated. The third grade non-Newtonian fluid subjected to the periodic body acceleration was employed. By employing the periodic pressure gradient, the pulsatile nature of the fluid flow was then examined. In order to differentiate the shear thinning/ thickening and the normal stress, the viscoelastic third grade non-Newtonian fluid model was adopted. The Caputo-Fabrizio time fractional model was solved by first taking the Laplace transformation followed by the finite Hankel transformation. While taking the inverse Laplace transformation, the Robotnov/Lorenzo function was used as well. The numerical results agreed well with those reported by Akbarzadeh [4] as shown in Table 1. The effects of magnetic field, third grade non-Newtonian fluid parameter, Womersely number and porosity parameter on the axial velocity were analyzed using the Mathematica software. The results are beneficial to the understandings of magnetic drug transportation in arteries, complex bio-waste fluids deliveries, irregularities of gastro intestinal regulated by magnetic field, magneto endoscopy and surgeries in bleeding control.

2. Formulation of the problem

The unsteady pulsatile laminar MHD flow of the third grade incompressible non-Newtonian fluid inside the porous artery was analyzed. The problem domain in the cylindrical coordinate systems (r, ϕ, x) was shown in Figure (1). As seen, blood flows in the x-direction through a porous artery of radius R, The axial blood flow velocity *u(r, t)*. The fluid flow was axisymmetric. On the outer wall (i.e. $r = R$), the no-slip condition ($u = 0$) was assumed. Due to the pumping action of heart, the pressure gradient was included to simulate the pulastile blood flow inside the porous artery,

$$-\frac{\partial p}{\partial x} = A_{g0} + A_{g1}\cos(\omega_p t), g(t) = A_g \cos(\omega_g t + \vartheta). \quad (1)$$

In (1), A_{g0} is the steady part and A_{g1} is the amplitude of the pressure fluctuation that gives rise to the systolic and diastolic pressures. $\omega_p = 2\pi f_p$ is the frequency of the heart pressure, and f_p is the frequency of the pulse rate. Furthermore, *g(t)* represents the body acceleration, A_g is the acceleration amplitude, ω_g is the frequency, and ϑ is the angle between the body acceleration and the pressure gradient. The effect of gravity was neglected.

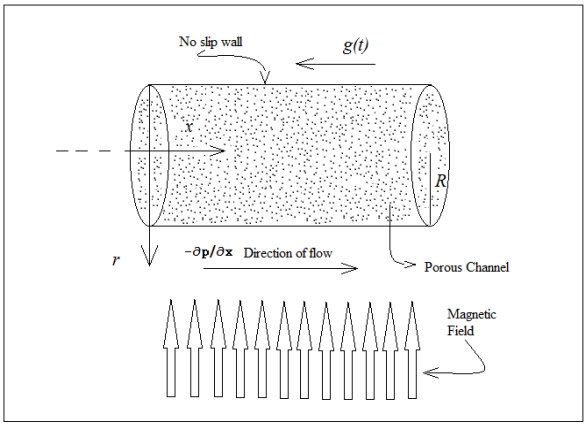

Fig. 1: Flow pattern

The governing momentum equation in the axial direction (Akbarzadeh [4]) can be written as:

$$\rho\frac{\partial}{\partial t}u(r,t) = -\frac{\partial p}{\partial x}\{div\tau\}_x - \frac{\mu}{K}u(r,t) - \rho A_g \cos(\omega_g t + \vartheta) - \sigma B_0{}^2 u(r,t), \quad (2)$$

where $\tau = pI + [\mu + \beta(t A_1{}^2 r)]A_1 + \alpha_1 A_2 + \alpha_2 A_1{}^2$, τ is the stress tensor, p is the pressure, K is the porosity parameter, μ is the blood viscosity, ρ is the blood density, $\sigma B_0{}^2$ is the magnetic parameter, t is the time, α_1, α_2 and β are the material moduli, and A_1 and A_2 are the Rivlin Ericksen or kinematical tensors

$$A_1 = \begin{pmatrix} 0 & 0 & \frac{\partial u}{\partial r} \\ 0 & 0 & 0 \\ \frac{\partial u}{\partial r} & 0 & 0 \end{pmatrix}, \; A_2 = \begin{pmatrix} 2\left(\frac{\partial u}{\partial r}\right)^2 & 0 & 0 \\ 0 & 0 & 0 \\ 0 & 0 & 0 \end{pmatrix}. \quad (3)$$

The non-dimensional variables are,

$$r' = \frac{r}{R}, u' = \frac{u}{U_\infty}, t' = \frac{\omega_p t}{2\pi}. \quad (4)$$

The dimensionless form of the momentum equation (2), can be written as,

$$\zeta^2 \frac{\partial}{\partial t}u(r,t) = B_1(1+\gamma\cos 2\pi t) + \left(\frac{1}{r}\frac{\partial}{\partial r}u(r,t) + \frac{\partial^2}{\partial r^2}u(r,t)\right) + \Lambda\left\{\frac{1}{r}\left(\frac{\partial}{\partial r}u(r,t)\right)^3 + 3\frac{\partial^2}{\partial r^2}u(r,t)\left(\frac{\partial}{\partial r}u(r,t)\right)^2\right\} + B_2\cos(2\pi\omega t+\vartheta) - (M^2+P)u(r,t). \quad (5)$$

The Caputo-Fabrizio time fractional model of order α of (5) such that $\alpha \in (0,1)$ obtained by taking $\frac{\partial}{\partial t} = D_t^{(\alpha)}$,

$$\zeta^2 \frac{\partial}{\partial t}u(r,t) = B_1(1+\gamma\cos 2\pi t) + \left(\frac{1}{r}\frac{\partial}{\partial r}u(r,t) + \frac{\partial^2}{\partial r^2}u(r,t)\right) + \Lambda\left\{\frac{1}{r}\left(\frac{\partial}{\partial r}u(r,t)\right)^3 + 3\frac{\partial^2}{\partial r^2}u(r,t)\left(\frac{\partial}{\partial r}u(r,t)\right)^2\right\} + B_2\cos(2\pi\omega t+\vartheta) - (M^2+P)u(r,t), \quad (6)$$

where $\zeta^2 = \frac{\rho\omega_p R^2}{2\pi\mu}$ is the dimension less Womersley number, $\gamma = \frac{A_0}{A_1}$ and $\Lambda = \frac{2\beta {U_\infty}^2}{\mu R^2}$ are the third grade non Newtonian fluid parameters, $B_1 = \frac{A_0}{\mu U_\infty}$ represents the pressure gradient, $M^2 = \frac{\sigma {B_0}^2}{\mu}$ is the magnetic field parameter, and $B_2 = \frac{\rho A_g R^2}{\mu U_\infty}$ shows the acceleration parameter. The, frequency ratios can be represented as $\omega = \frac{\omega_g}{\omega_p}$ and $\frac{B_2}{B_1} = \frac{\rho A_g}{A_0}$. Furthermore,

$$D_t^{(\alpha)} f(t) = \frac{M(\alpha)}{1-\alpha}\int_a^t \dot{f}(\tau)e^{-\frac{\alpha(t-\tau)}{1-\alpha}}d\tau, \quad (7)$$

with $\alpha \in [0,1]$, $a \in [-\infty, t)$ and $f \in L^1(a,b), b > a$, where $L^1(a,b)$ is the class of all integrate able functions f on $[a,b]$. $M(\alpha)$ is the normalization function such that $M(0) = M(1) = 1$. In the current paper, the condition $\alpha \in (0,1)$ was followed strictly in order, to have a better understanding on the problem of the non-local model. For $\alpha = 1$, the non-locality was lost. The non-dimensional initial and boundary conditions can be written as:

$$\left.\begin{array}{l} u(r,0) = 0 \\ \frac{\partial}{\partial r}u(r,t)|_{r=0} = 0 \\ u(1,t) = 0 \end{array}\right\}. \quad (8)$$

3. Solution to the problem

The new definition of Caputo-Fabrizio fractional derivative (NFD$_t$) assumes two different representations for the temporal and spatial variables. The first representation works on time variable. In this situation it is more convenient to use the Laplace transform. By applying the Laplace transform on the temporal variable *t* given in (6) and imposing the boundary conditions given in (8):

$$\zeta^2 \frac{s\bar{u}(r,s)}{s+\alpha(1-s)} = B_1\left(1+\gamma\frac{s}{s^2+4\pi^2}\right) + \left(\frac{1}{r}\frac{\partial\bar{u}(r,s)}{\partial r} + \frac{\partial^2\bar{u}(r,s)}{\partial r^2}\right) + \Lambda\left\{\frac{1}{r}\left(\frac{\partial\bar{u}(r,s)}{\partial r}\right)^3 + 3\frac{\partial^2\bar{u}(r,s)}{\partial r^2}\left(\frac{\partial u(r,s)}{\partial r}\right)^2\right\} - (M^2+P)\bar{u}(r,s) + B_2\left(\frac{s\cos\vartheta - 2\pi\omega\sin\vartheta}{s^2+4\pi^2\omega^2}\right), \quad (9)$$

$$\left.\begin{array}{l} \bar{u}(r,0) = 0 \\ \frac{\partial}{\partial r}\bar{u}(r,s)|_{r=0} = 0 \\ \bar{u}(1,s) = 0 \end{array}\right\}. \quad (10)$$

Here $\bar{u}(r,s) = L[u(r,t)]$. The dimension-less governing Caputo-Fabrizio time fractional model contains highly non-linear terms with respect to the radial component *r*. By taking the finite Hankel transform of order zero with respect to the radial coordinate *r* of (9) and applying the boundary conditions in (10)

$$\bar{u}_H(r_n,s)\left[\zeta^2\frac{s}{s+\alpha(1-s)} + {r_n}^2(\Lambda+1) + M^2 + P\right] = \frac{J_1(r_n)}{r_n}\left[B_1\left(1+\gamma\frac{s}{s^2+4\pi^2}\right) + B_2\left(\frac{s\cos\vartheta - 2\pi\omega\sin\vartheta}{s^2+4\pi^2\omega^2}\right)\right], \quad (11)$$

where $\bar{u}_H(r_n,s) = H[\bar{u}(r,s)]$, r_n for $n = 1,2,...$, are the positive roots of the equation $J_0(x) = 0$, which is the Bessel function of first kind and zero order. Eq. (11) can be written explicitly for $\bar{u}_H(r_n,s)$ as

$$\bar{u}_H(r_n,s) = \frac{J_1(r_n)}{a_{n4}r_n}\left[B_1\left(\frac{s}{s+a_{n2}} + \gamma\frac{s}{s+a_{n2}}\times\frac{s}{s^2+4\pi^2} + \frac{a_{n3}}{s+a_{n2}} + \gamma\frac{a_{n3}}{s+a_{n2}}\times\frac{s}{s^2+4\pi^2}\right) + B_2\frac{s\cos\vartheta - 2\pi\omega\sin\vartheta}{s^2+4\pi^2\omega^2}\times\left(\frac{s}{s+a_{n2}} + \frac{a_{n3}}{s+a_{n2}}\right)\right]. \quad (12)$$

3.1. Axial velocity

By applying the inverse Laplace transform L^{-1} on (12) and using the Robotnov/Lorenzo $F_q[a, t]$ function defined as,

$$L^{-1}\left(\frac{1}{s^q - a}\right) = F_q[a,t] = \sum_{n=0}^{\infty}\frac{a^n t^{(n+1)q-1}}{\Gamma((n+1)q)}. \quad (13)$$

One obtains

$$u_H(r_n,t) = \frac{J_1(r_n)}{a_{n4}r_n}\left[B_1\left(-\gamma a_{n2}.e^{-a_{n2}t} * \cos 2\pi t + a_{n3}.e^{-a_{n3}t} - a_{n2}.e^{-a_{n2}t} + \gamma a_{n3}.e^{-a_{n2}t} * \cos 2\pi t\right) + B_2\left(-a_{n2}.e^{-a_{n2}t} * \cos(2\pi\omega t+\vartheta) + a_{n3}.e^{-a_{n2}t} * \cos(2\pi\omega t+\vartheta)\right)\right]. \quad (14)$$

By inverting the Hankel transformation in (14), the final expression for axial velocity, which has two Bessel functions with zero and first order of first kind, can be retrieved.

$$u(r,t) = 2\sum_{n=1}^{\infty} \frac{J_0(r\, r_n)}{J_1^{\,2}(r_n)} u_H(r_n,t), \tag{15}$$

$$u(r,t) = 2\sum_{n=1}^{\infty} \frac{J_0(r\, r_n)}{a_{n4}\, r_n\, J_1\,(r_n)} \Big[B_1 \Big(-\gamma\, a_{n2}.e^{-a_{n2}t} * \cos 2\pi t + a_{n3}.e^{-a_{n3}t} - a_{n3}.e^{-a_{n3}t} - a_{n2}.e^{-a_{n2}t} + \gamma\, a_{n3}.e^{-a_{n2}t} * \cos 2\pi t \Big) + B_2 \Big(-a_{n2}.e^{-a_{n2}t} * \cos(2\pi\omega t + \vartheta) + a_{n3}.e^{-a_{n2}t} * \cos(2\pi\omega t + \vartheta) \Big) \Big]. \tag{16}$$

The axial flow velocity in the domain of interest can be determined via (16). In (14) and (16), $f * g$ represents the convolution product of f and g. The parameters used in evaluating the simulation results are:

$$a_{n1} = \mathrm{M}^2 + \mathrm{P} + r_{n2}(1+\Lambda), \tag{17}$$

$$a_{n2} = \frac{a_{n1}\alpha}{\alpha_{12} + a_{n1} - a_{n1}\alpha}, \tag{18}$$

$$a_{n3} = \frac{\alpha}{1-\alpha}, \tag{19}$$

$$a_{n4} = \frac{a_{n1}\, a_{n3}}{a_{n2}}. \tag{20}$$

4. Results and discussion

The main aim of the current study was to apply the Caputo Fabrizio fractional derivative NFD_t for MHD blood flow simulation. The time fractional model was solved using $\alpha \in (0,1)$ to enforce non-locality. In order to compare the current results with those reported by Akbarzadeh [4], $\alpha = 1$ was taken and the governing equations were solved using the local model. As shown in the Table 1, good agreement was found. The fluid velocity $u(r,t)$ in the x-direction obtained from (16) was then examined by manipulating the values of Womersley number ζ, third grade non-Newtonian parameter Λ, magnetic field parameter M and porosity parameter P. The axial and radial velocity $u(r,t)$ profiles were plotted for $\alpha \in \{0.2, 0.3, 0.5\}$ (see Figures (2-13)). In these plots the following parameters were prescribed: $B_1 = 1.4, B_2 = 1.44$, $\gamma = 0.2, \omega = 1$, $\vartheta = \frac{\pi}{24}$ and $t = 1.939$.

By increasing the strength of the external magnetic field, the radial flow speed decreased. Therefore, by simply controlling the external magnetic field, the axial blood flow velocity can be adjusted accordingly. The effect of the intensity of external magnetic field on the blood flow velocity was depicted in Figures (2-4). Moreover, the velocity variation was large at higher fractional parameter α.

Figures (5-7) show the influence of the third grade parameter Λ on the flow behavior. As seen, the amplitude of the velocity profile decreased as the third grade non-Newtonian parameter Λ increased, which was consistent to that reported by Akbarzadeh [4]. The effect of Womersley number ζ (ratio of transient inertial to viscous forces) on the axial velocity was depicted in Figures (8-10). At large ζ, the velocity profile was parabolic, indicating that the fluid was dominated by the inertial forces. At small ζ, the velocity decreased with respect r, (viscous dominated). However, for large ζ, a small variation was observed when the fractional parameter α approached null. The correlation between the permeability parameter P and the velocity was negative as shown in Figures (11-13) due to the porous nature of the channel or artery. This observation is helpful in surgeries.

5. Conclusion

The pulsatile blood flow inside the porous arteries was simulated by applying exerting the periodic pressure gradient (simulating the presence of an external magnetic field). The Caputo-Fabrizio (NFD_t) time fractional order derivative was adopted. The blood was modeled as the third-grade non-Newtonian fluid. The time fractional model was solved by first taking the Laplace transformation, followed by the finite Hankel transformation (coupled with the Lorenzo function). The governing time fractional model was solved in the non-local system. The relationship between the velocity and the α value was investigated for various flow parameters. The correlation between the velocity and variables such as the visco-elastic, the magnetic field and the porosity parameters were negative. Nevertheless, the velocity increased with respect to the Womersely number. The simulated velocity profile agreed well with that reported previously. The current findings are helpful in the clinical investigations of various arterial diseases.

Acknowledgement

I would like to acknowledge the financial aid received from the Research, Innovation, Commercialization and Consultancy Management (ORICC) under Tier 1/H070 grant and Centre for Graduate Studies Universiti Tun Hussein Onn Malaysia. I would also like to express my sincere gratitude to Dr. Mahathir Bin Mohamad and Prof. Dr. Rozaini Bin Roslan for the continuous support, patience and motivation for my research work.

Table 1: Comparison between NFD_t and Akbarzadeh [4]

Serial Number	$u(r, t)$ was calculated by taking $\mathrm{M}^2+\mathrm{P}=0$ and $\alpha = 1$	
	Akbarzadeh [4]	NFD_t
1.	0.1165	0.1178
2.	0.1192	0.1193
3.	0.1184	0.1189
4.	0.1176	0.1184
5.	0.1170	0.1181
6.	0.1198	0.1196
7.	0.1225	0.1211
8.	0.1527	0.1507

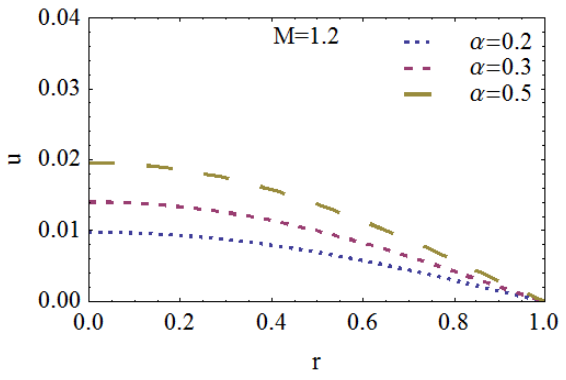

Fig.2. Axial velocity for different values of α and at $\mathrm{M} = 1.2$ against r

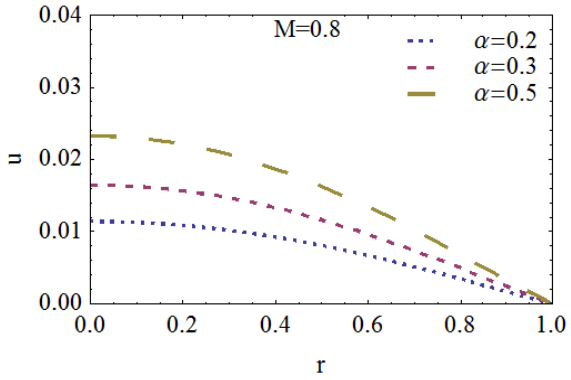

Fig.3. Axial velocity for different values of α and at $M = 0.8$ against r

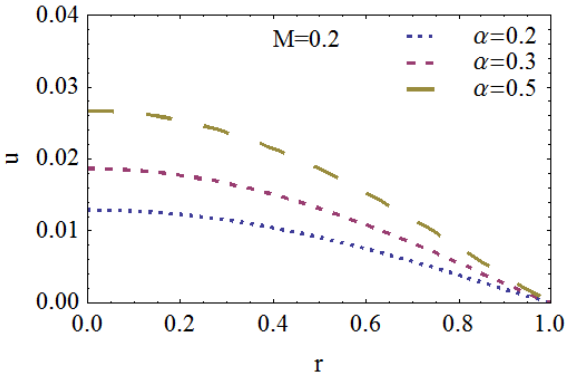

Fig.4. Axial velocity for different values of α and at $M = 0.2$ against r

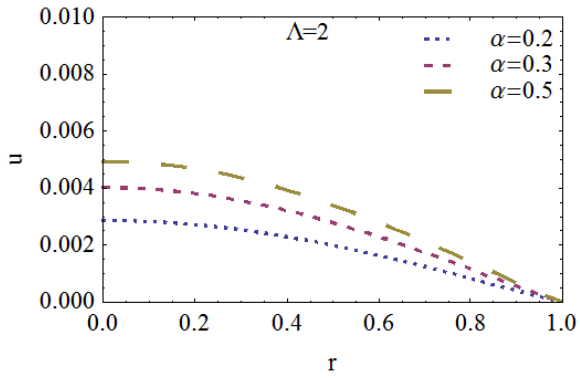

Fig.5. Axial velocity for different values of α and at $\Lambda = 2$ against r

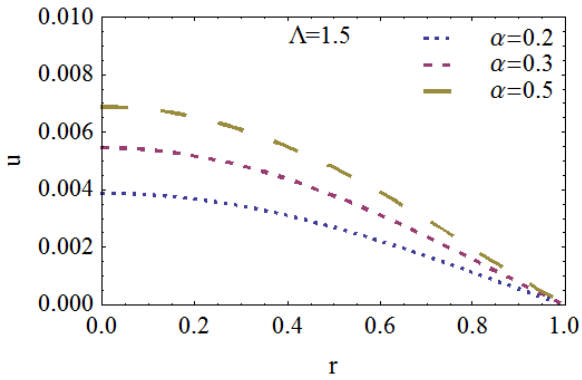

Fig.6. Axial velocity for different values of α and at $\Lambda = 1.5$ against r

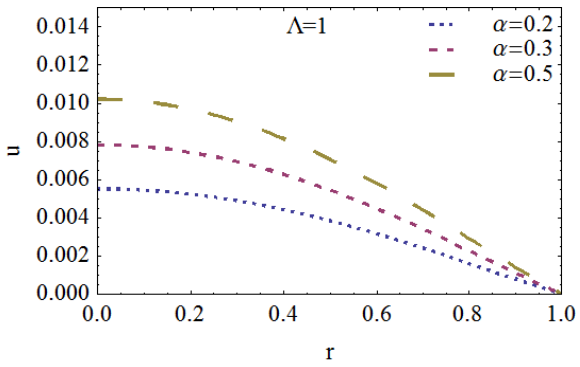

Fig.7. Axial velocity for different values of α and at $\Lambda = 1$ against r

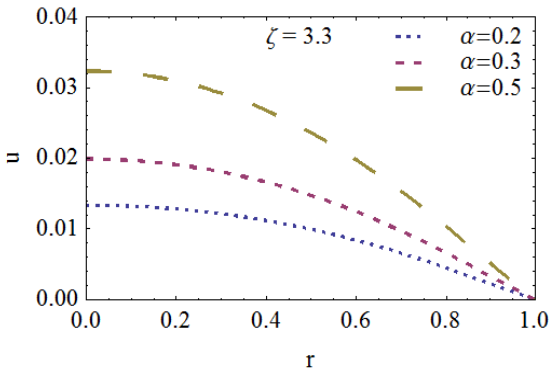

Fig.8. Axial velocity for different values of α and at $\zeta = 3.3$ against r

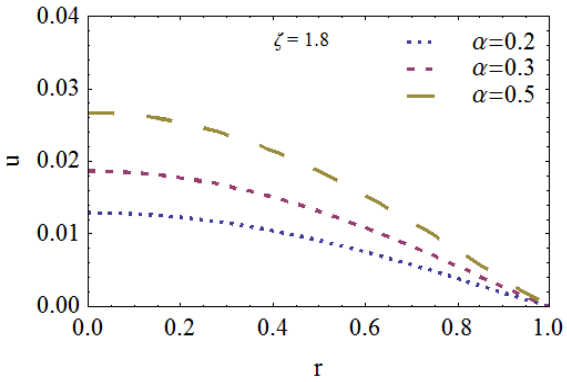

Fig.9. Axial velocity for different values of α and at $\zeta = 1.8$ against r

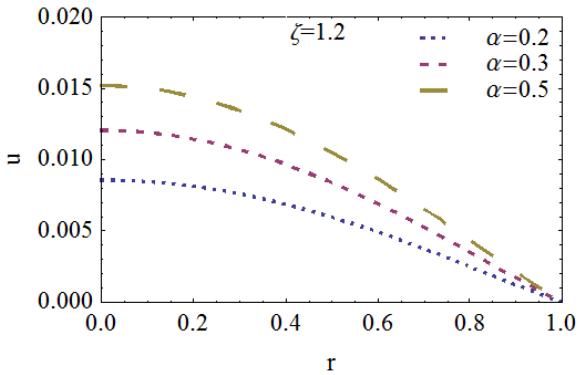

Fig.10. Axial velocity for different values of α and at $\zeta = 1.2$ against r

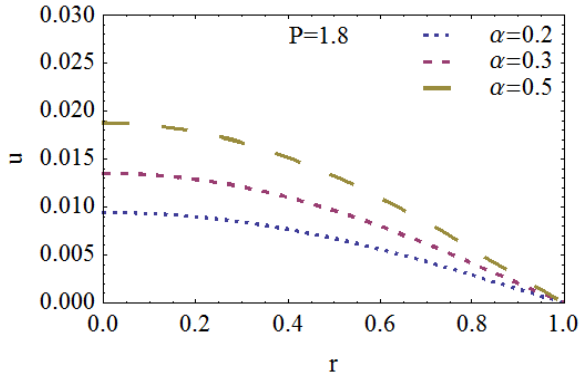

Fig.11. Axial velocity for different values of α and at $P = 1.8$ against r

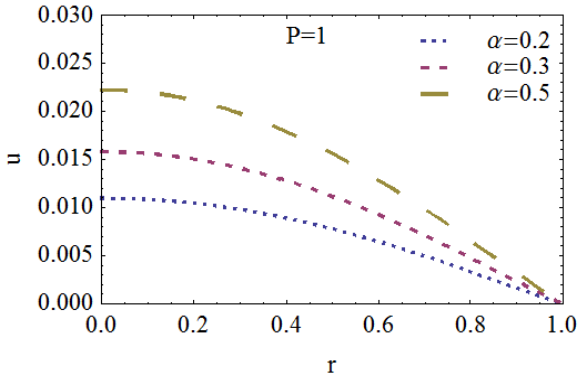

Fig.12. Axial velocity for different values of α and at $P = 1$ against r

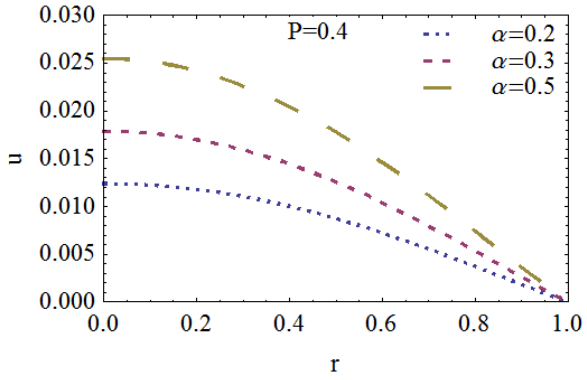

Fig.13. Axial velocity for different values of α and at $P = 0.4$ against r

References

[1] Abdullah M, Rashid A, Raza N, Saleh A, & Alzahrani AK (2018), Analysis of blood flow with nanoparticles induced by uniform magnetic field through a circular cylinder with fractional caputo derivatives, *J. of Mag. and Mag. Mater.*, 446, pp.28–36

[2] Akbar NS (2016), Non-Newtonian model study for blood flow through a tapered artery with a stenosis, *Alex. Eng. J.*, 55(1), pp.321–329

[3] Akbar NS & Nadeem S (2014), Carreau fluid model for blood flow through a tapered artery with a stenosis, *Ain. Shams. Eng. J.*, 5(17), pp.1307–1316

[4] Akbarzadeh P (2016), Pulsatile magneto-hydrodynamic blood flows through porous blood vessels using a third grade non-Newtonian fluids model, *Com. Methods. and Prog. in Biomed.*, 126, pp.3–19

[5] Akinshilo AT & Sobamowo GM (2017), Perturbation solutions for the study of mhd blood as a third grade nano fluid transporting gold nanoparticles through a porous channel, *J. of App. And Comp. Mech.*, 3(2), pp.103–113

[6] Bao S, Zhang R, Wang K, Zhi X & Qiu L (2017), Free surface flow of liquid oxygen under non-uniform magnetic field, *Cryogenics.*, 81, pp.76-82

[7] Das UJ (2013), Viscoelastic effects on unsteady two-dimensional and mass transfer of a viscoelastic fluid in a porous channel with radiative heat transfer, *Eng*., pp.67–72

[8] Eldesoky IM (2012), Mathematical analysis of unsteady MHD blood flow through parallel plate channel with heat source, *W. J. of Mech.*, pp.131–137

[9] Fardad AA, Sedaghatizadeh M, Sedaghatizadeh N & Soleimani S (2011), Temperature, velocity and micro rotation analysis of blood flow in cosserat continuum using homotopy perturbation method, *Wor. App. Sci. J.*, 14(7), pp.1042–1047

[10] Gupta AK & Agrawal SP (2015), Computational modeling and analysis of the hydrodynamic parameters of blood through stenotic artery, *Pro. Comp. Sci.*, 57, pp.403–410

[11] Krasnov D, Zikanov O & Boeck T (2011), Comparative study of finite difference approaches in simulation of magnetohydrodynamic turbulence at low magnetic Reynolds number, *Comp. and Fluids*, 50(1), pp.46–59

[12] Mekheimer KS & Kot MAE (2015), Engineering science and technology, an international journal suspension model for blood flow through catheterized curved artery with time-variant overlapping stenosis, *Eng. Sci. and Tech. an Int. J.*, 18(3), pp.452–462

[13] Okuyade WIA (2013), On the pressure velocity and temperature factors and the effect of viscosity on the arterial blood flow in relation to the hypertension patient, part-1, flow without out flow, *Afr. J. Sci. Tech.*, 12(2), pp.99–104

[14] Parmar A & Jain S (2017), Comparative study of flow and heat transfer behavior of Newtonian and non-Newtonian fluids over a permeable stretching surface, *Gl. and Sto. Ana*., 25, pp.41–50

[15] Ram P, Kumar A & Singh H (2013), Effect of porosity on unsteady MHD flow past a semi-infinite moving vertical plate with time dependent suction, *Ind. J. of Pur. and App. Phy.*, 51, pp.461–470

[16] Singh J & R. Rathee (2010), Analytical solution of two-dimensional model of blood flow with variable viscosity through an indented artery due to LDL effect in the presence of magnetic field, *Int. J. of the. Phy. Sci.*, 5(12), pp.1857–1868

[17] Venkateswarlu K & Rao JA (2004), Numerical solution of unsteady blood flow through an indented tube with atherosclerosis, *Ind. J. of Bioch. and Biophy.*, 41, pp.241–245